MRI study of the posterior visual pathways in primary open angle glaucoma

Wei Zhou, PhD, **Eric R Muir, PhD**, **Steven Chalfin, MD**, **Kundandeep S Nagi, MD**, and **Timothy Q Duong, PhD**

Department of Ophthalmology, Research Imaging Institute, University of Texas Health Science Center, San Antonio, TX, 78229

Abstract

Purpose—To evaluate neurodegeneration along brain visual pathways in primary open angle glaucoma (POAG) using improved analysis methods of volumetric and diffusion-tensor MRI data.

Methods—Eleven POAG patients (60.0±9.2yo) with primarily mild to moderate POAG and eleven age-matched controls (55.9±7.5yo) were studied using structural and diffusion-tensor MRI. Surface-based segmentation was applied to structural MRI to obtain visual cortical area and volume. Fiber tracking was applied to diffusion-tensor data to obtain diffusion parameters along the optic tract and optic radiation. MRI parameters in glaucoma patients were compared with the corresponding left and right visual fields and retinal nerve fiber layer thicknesses, instead of with the left and right eye.

Results—Area and volume of the primary visual cortex were significantly reduced in POAG patients compared to controls (P<0.05) but did not correlate with visual field loss. Fractional anisotropy was reduced at multiple locations along the optic tracts and optic radiations in POAG patients compared to controls. Axial and radial diffusivity along the fiber tracts showed trends but were not significantly different between POAG patients and controls when averaged over the whole structures. Only fractional anisotropy (P<0.05) of the optic radiations were significantly correlated with visual field loss. No MRI parameters were correlated with retinal nerve fiber layer thickness.

Conclusions—Improved analysis techniques of MRI data improves delineation of degeneration in the brain visual pathways and further supports the notion that neurodegeneration is involved with glaucoma pathogenesis.

Keywords

Fractional anisotropy; retinal nerve fiber layer; diffusion tensor imaging; visual field; magnetic resonance imaging

Correspondence: Timothy Q Duong, PhD, University of Texas Health Science Center at San Antonio, Department of Ophthalmology, 8403 Floyd Curl Dr, San Antonio, TX 78229. Phone: 210-567-8474. duongt@uthscsa.edu.

The authors declare no conflict of interest.

Introduction

Glaucoma is a leading cause of irreversible blindness that afflicts more than 4 million Americans.[1] The eventual outcome is often blindness, starting with loss of peripheral vision followed by loss of central vision. Glaucoma is characterized by cupping of the optic nerve head and thinning of the retinal nerve fiber layer (RNFL) due to loss of retinal ganglion cells, which becomes evident only after a substantial number of retinal ganglion cells have already died.[2–5] Visual field measurements and RNFL thickness are often used to gauge the progression of vision loss and glaucoma severity. Elevated intraocular pressure (IOP) is a known risk factor, and lowering IOP is the only available treatment for glaucoma.[6] However, many glaucoma patients continue to lose vision despite successful medical or surgical treatment to lower IOP.[7] As such, there are likely other factors that contribute to the disease progression.

Neurodegeneration and trans-synaptic degeneration in the optic nerve, optic tract, lateral geniculate nucleus, optic radiation, and visual cortex have been reported in glaucoma.[3,8–11] Axonal damage of the retinal ganglion cells has been suggested to precede the loss of cell bodies.[12] Shrinkage of the lateral geniculate nucleus has been documented in ocular hypertension in the absence of optic nerve fiber loss.[8] Oxidative damage and glutamate toxicity have been implicated in trans-synaptic central nervous system injury in glaucoma.[11] As damage to the lateral geniculate nucleus and visual cortex can induce loss of retinal ganglion cells, degeneration in the posterior visual pathway could contribute to disease progression in glaucoma.[9]

Recent MRI studies have provided further evidence of neurologic damage in glaucoma. Morphometric MRI studies found atrophy in the lateral geniculate nuclei[13,14] and visual cortex,[15,16] optic nerve, optic chiasm, optic tract, and optic radiation[17] in glaucoma patients. Diffusion tensor imaging (DTI) MRI studies found altered diffusivity and fractional anisotropy of the optic radiation and optic nerve in glaucoma.[15,18–21] Abnormal DTI parameters[20,22] have been shown to correlate with glaucoma severity.[19] The majority of the previous studies employed voxel-based group analysis, which may not adequately pinpoint atrophy to specific regions in the brain. Moreover, previous studies of glaucoma patients compare MRI parameters with visual field loss of the left and right eyes (not left and right visual fields) whereas the visual pathways are segregated by visual field after the optic chiasm and thus the unilateral posterior visual pathway receives input from the ipsilateral retina and the contralateral visual field from both eyes. However, such correct comparison has not been made. In addition, comparison of MRI parameters with left and right visual fields (instead of left and right eyes) could also improve delineation of neurodegeneration in glaucoma.

The goal of this study was to employ improved analysis methods of volumetric and diffusion-tensor MRI to evaluate changes in the optic tract, optic radiation, and primary visual cortex in POAG patients. Primarily mild and moderate POAG patients were studied and compared with age-matched controls. Glaucomatous damage in the left and right cerebral hemispheres were analyzed with respect to the corresponding visual field loss of the contralateral visual hemifields.[23] Moreover, in contrast to most previous studies, which used

voxel-based group analysis, a novel algorithm[24] was employed to map the spatial profiles of the white matter tracts of the visual pathway of individual subjects. This study explored the hypothesis that with sophisticated analysis techniques, volumetric and diffusion-tensor MRI will allow improved substructural delineation of neurodegenerative pathogenesis in the brain visual pathways.

Methods

Subjects

This study was approved by the local Institutional Review Board. Informed consent was obtained for all participants. Eleven patients with diagnosed primary open angle glaucoma (POAG) (age range: 36–72 yo, average: 60.0±9.2 yo, 4 males) and eleven healthy age-matched adults (age range: 37–65 yo, average: 55.9±7.5 yo, 7 males) were enrolled in the study. The clinical diagnosis of POAG was performed or confirmed by two qualified ophthalmologists (SC and KN). The glaucoma diagnosis was made based on the diagnostic criteria of the American Academy of Ophthalmology's Glaucoma Primary Open-Angle Glaucoma Preferred Practice Pattern® Guidelines[25] through assessment of the open anterior chamber angle, identification of visual field defects typical of glaucoma, optic disc cupping, or identification of an IOP of 21 mmHg or greater. Exclusion criteria were any retained metallic foreign body or implanted device, history of claustrophobia, neurological or psychiatric disorders, diabetes, eye surgery, other eye diseases (except near-sightedness), and clinically abnormal structural brain MRI. Severity of glaucoma was categorized as mild, moderate and severe based on established criteria.[25,26] Normal controls were age-matched participants free of all eye diseases with the same exclusion criteria.

Clinical data

Glaucoma patients underwent standard clinical eye exams, which included visual field scores by automated perimetry (HFA II 750, Carl Zeiss, Dublin, CA), intraocular pressure by tonometry (Goldmann applanation, Haag-Streit Diagnostics, Bern, Switzerland), and retinal nerve fiber layer thickness by optical coherence tomography (Spectralis, Heidelberg Engineering, Heidelberg, Germany) for glaucoma diagnosis. The pattern standard deviation (PSD) values of both right and left eyes were the standard outputs of the visual field tests. The visual pathways of the two eyes are combined by visual field after the optic chiasm and thus the unilateral posterior visual pathway receives input from the ipsilateral retina and the contralateral visual field from both eyes. Thus, it is necessary to combine visual data when compared with brain data. For such comparison with individual brain hemispheres, for each patient, the PSD values of right and left eyes were combined point by point by taking either the "mean" and the "best" value of the two eyes[27,28] to obtain binocular visual fields, and then separated by right and left visual fields, and averaged over each hemifield. Similarly, right and left RNFL thickness hemispheric values from the monocular OCT data were obtained from combining unilateral hemispheres of RNFL thickness of two eyes. The "mean" and the "best" location algorithm yielded similar results and conclusions when correlated with MRI data, and thus only the "mean" algorithm results were presented.

MRI Acquisition

MRI data were acquired using a 3-Tesla scanner (Magnetom Trio, Siemens, Erlangen, Germany) with a standard 8-channel head coil. Brain anatomical MRI was obtained using a T1-weighted MP-RAGE sequence for the whole brain with repetition time TR = 2200 ms, echo time TE = 2.8 ms, field of view FOV = $176 \times 256 \times 208$ mm, matrix size $=176 \times 256 \times 208$, bandwidth = 190 Hz/pixel, flip angle = 13°, and scan duration = 3 min. DTI was acquired using a single spin echo, twice refocused, echo planar imaging diffusion sequence covering the entire visual pathway of each subject. The parameters were: TR = 6000 ms, TE = 90 ms, FOV = $192 \times 192 \times 92$ mm, matrix size = $64 \times 64 \times 46$, with 64 directions at b = 1000 s/mm^2 and one b = 0 s/mm^{2,29} bandwidth = 1420 Hz/pixel, and scan duration = 6.5 min.

MRI Image Processing

T1-weighted anatomic images were first aligned to the anterior commissure – posterior commissure (AC-PC) plane and were processed in Freesufer (https://surfer.nmr.mgh.harvard.edu) to derive cortical and non-cortical parcellations including the optic chiasm and primary visual cortex (V1). Gray matter surface reconstruction of cortical regions was then performed to obtain the cortical volume and surface area of V1.

Diffusion MRI images were processed in MATLAB (Math works, Natick, MA, USA) using the mrDiffusion package (https://github.com/vistalab/vistasoft/mrDiffusion) with eddy-current correction and motion correction. The corrected non-diffusion image was aligned to the T1-weighted images in the AC-PC space. The eigenvalues from the diffusion tensor, fractional anisotropy (FA), radial diffusivity (RD), axial diffusivity[3] and mean diffusivity (MD) were calculated.

Fiber tract profiles of the optic tract and optic radiation for both hemispheres were segmented using probabilistic fiber tracking (https://github.com/jyeatman/AFQ).[24] To identify the optic tract and optic radiation, regions of interest (ROIs) of the optic chiasm and V1 were obtained from automatic segmentation of the T1-weighted anatomic image in Freesurfer. For the lateral geniculate nuclei (LGN) ROIs, 5 mm spheres for both hemispheres were manually defined lateral to the hypothalamus on the high-resolution anatomical images.[30] The LGN ROIs were adjusted and confirmed by ensuring that they covered the endpoints of fibers from the optic chiasm. Fibers were "cleaned" by removing outliers and gray matter components.[24] Taking tract length into consideration, 30 or 100 nodes[31] were taken along the cleaned individual optic tract or optic radiation segments, respectively. Five nodes at the ends of each track were removed to avoid partial volume artifacts. Each diffusion measure (FA, RD, AD, and MD) was averaged at each node along the two tracts of the two hemispheres and rendered onto the tract profile. The spatial profiles of diffusion measures were plotted as function of distance.

Statistical analysis

For gray matter area and volume of the V1, group comparisons were assessed by ANCOVAs with intracranial volume as a covariate factor (to regress the effects of head size). The POAG patients' V1 area and volume data per brain hemisphere were correlated to corresponding

visual field scores or RNFL thicknesses, as well as head size, using multiple linear regressions. Mixed effects ANOVA (group as fixed effect, subject and hemisphere as random effect) was applied to compare diffusion parameters for all nodes as well as the group mean values of the entire optic tract and optic radiation between normal and POAG groups. Diffusion measures per brain hemisphere were correlated with corresponding left and right visual field scores and RNFL thicknesses using Spearman correlation. A threshold of $p < 0.05$ was considered statistically significant unless otherwise specified.

Results

Demographic data of POAG patients, their visual field PSD, IOP and average RNFL thickness are given in Table 1. There was no significant age difference between controls and glaucoma patients ($p > 0.05$). IOPs of POAG patients were within normal physiological ranges (<21 mmHg) as they were under standard clinical care, except one newly diagnosed POAG patient who had elevated IOP (#5). Visual field scores of the majority of POAG patients were abnormal compared to the age-corrected normal population database. RNFL thicknesses of the majority of POAG patients were abnormal compared to the normative database. Severity of glaucoma ranged from mild to moderate, except one patient, who was diagnosed as having severe glaucoma.

Figure 1 shows a representative visual field test from the left and right eyes of a POAG patient, which were combined to give a binocular visual field using the "mean" and "best" of the two eyes. Darker shade and more negative values indicate worse visual deflect. The binocular visual field clinical data were converted to the left and right visual field scores, which were used for correlation with MRI data per corresponding brain hemisphere.

The surface area and volume of the V1 of POAG patients were significantly reduced compared to age-matched controls ($p < 0.01$, ANCOVA, Figure 2). V1 area and V1 volume of the POAG patients however showed no significant correlation with disease severity as indicated by visual field scores (V1 area: Multiple $R^2 = 0.212$, $p > 0.05$; V1 volume: Multiple $R^2 = 0.060$, $p > 0.05$).

Figure 3 shows the seed ROIs used for DTI analysis and the resulting fiber tracts. Seeds for fiber tracking were placed in the optic chiasm, lateral geniculate and primary visual cortex from which fiber tracts and diffusion indices of the optic tract and optic radiation were derived. FA spatial profiles along the optic tract and optic radiation are plotted for POAG and control subjects (Figure 4). FA in the optic tract close to the optic chiasm and LGN (node 1–3, 12–14, $p < 0.05$; shaded regions) showed significant differences between POAG and control group. The FA in the optic radiation near the middle of the tract and close to V1 (node 30–37, 47–48,75–80, 87–88, $p < 0.05$; node 39–46, 81–86, $p < 0.01$; shaded regions) showed significant differences between POAG and controls. The group mean FA values of the entire optic tract and optic radiation in the POAG group were significantly reduced (optic tract, $p < 0.05$; optic radiation, $p < 0.01$) compared with age-matched controls. FA of the optic tract did not correlate with visual field scores in POAG patients ($R = 0.145$, $p > 0.05$), whereas FA of the optic radiation did ($R = 0.537$, $p < 0.05$).

Radial diffusivity, axial diffusivity, and mean diffusivity profiles of the optic tract and optic radiation and their group means are displayed in Figure 5. Radial diffusivity showed a trend of being increased in POAG patients compared to controls in the optic radiation with node 43 and 75–76 showing significant difference ($p < 0.05$). Axial diffusivity showed a trend of decreasing in POAG patients compared with controls in the optic tract with node 17–19 showing significant difference ($p < 0.05$). Mean diffusivities were not significantly different between POAG patients and controls in neither the optic tract or optic radiation. None of the diffusivity of the optic tract or optic radiation was significantly correlated with visual field data ($p > 0.05$).

None of the MRI parameters were significantly correlated with RNFL thickness ($p > 0.05$). Visual field scores were also not significantly correlated with RNFL thickness ($p > 0.05$). None of the MRI parameters were significantly correlated with IOP ($p > 0.05$) as expected because IOPs of all but one POAG patient were maintained within normal physiological ranges by standard clinical treatments in our study.

Discussion

This study evaluated glaucomatous damage along visual pathways of the brain using novel analysis approaches of volumetric and diffusion tensor MRI data. In contrast to the majority of previous studies that employed voxel-based group analysis, we used surface-based segmentation of gray matter and a novel algorithm to map the spatial profiles of the white matter tracts of the visual pathway on individual patient data. We also compared glaucomatous visual field loss from the left and right hemifield (instead of typical left and right eye) with gray matter and white matter from the corresponding contralateral hemispheres. The major findings in the present study are: i) the visual cortex area and volume are significantly reduced in POAG patients compared to age-matched controls but they do not correlate with disease severity in mild to moderate POAG patients, ii) fractional anisotropy of the optic tract and optic radiation is reduced at multiple locations along the fiber tracts in POAG patients compared to controls. Radial, axial and mean diffusivity show trends between POAG patients and controls but did not reach overall statistical significance. Only the fractional anisotropy and radial diffusivity of optic radiations significantly correlate with the severity of visual field loss. These results lend credence to MRI as a potential biomarker for glaucoma staging, and support the notion that there is neurodegenration in the brain visual pathways of POAG patients.

V1 area and volume

V1 gray matter area and volume were significantly different between POAG patients and normal controls using surface-based segmentation methods. Our results corroborated previous voxel-based morphometry (VBM) reports on volumetric reduction of human visual cortex.[15,16] Another study however only found trends of reduced area and volume of V1 area and volume in glaucoma, but head size was not taken into account as a covariate.[32] Accounting for head size is likely important to detect differences as has been shown to be the case in the analysis of Alzheimer's disease.[33] A possible explanation for the gray matter degeneration is that the loss of visual function in glaucoma leads to fewer neural signals to

the visual cortex from the retina and other brain regions, resulting in the disuse-driven atrophy or shrinkage of neurons. The exact mechanism of the distal gray matter (V1) atrophy in glaucoma remains to be investigated.

While there were significant differences between glaucoma and control groups, we found gray matter area and volume did not correlate with disease severity as measured by visual fields in glaucoma patients. Similar studies of late blindness have also found no correlation between V1 volumetric atrophy and blindness duration.[34,35] It is possible that visual cortex atrophy may occur at a relatively early stage of vision loss but does not progress. Another possible explanation for the lack of correlation is the narrow dynamic range of disease severity in our study, which included only mild and moderate glaucoma (except one severe glaucoma patient).

White matter changes

FA of the optic tract and optic radiation was reduced in glaucoma patients, in general agreement with previous reports.[18,20,22,36] Conventional voxel based morphometry[15,20] and tract-based spatial statistics[37] analysis showed the spatial pattern of diffusion changes, although both techniques relied on precise cross-subject registration to yield statistical maps that highlighted differences between groups.[24,38] Imperfect image registration and inter-subject variation in tract shapes and locations could lower the precision and sensitivity. Other DTI studies of glaucoma reported only the overall mean FA values of the entire white matter tracts by ROI analysis.[18,22]

We used a different method of analysis in which FA abnormality along the length of the optic tract and optic radiation profiles were analyzed on an individual basis. Differences between groups were detected in the optic tract in both proximal and distal regions and in the optic radiation in the middle and near V1 regions. Brain diseases can affect different regions of brain substructures in a time- and disease-specific manner, and thus it is important to study these brain substructures. This method could be applied to individual glaucoma patients for assessment of optic tract and optic radiation profiles and compared with a normal population database.

The factors that contributed to FA changes may differ between the optic tract and optic radiation. FA difference along the optic tract was associated with reduced AD in glaucoma, whereas FA difference along the optic radiation was associated with increased RD. In the white matter structures, the myelin sheath wrapping around the axons does not constrain diffusivity along the fibers[3], whereas it does restrict diffusion perpendicular to the fibers (RD).[39] Thus, for glaucoma, decreased FA associated with reduced AD in optic tracts could reflect more general axonal degeneration, where the decreased FA associated with increased RD in optic radiations could reflect demyelination.[40] Further studies are needed to explore this hypothesis. FA changes of both optic tract and optic radiation in our study are consistent with previously reported DTI results in Leber hereditary optic neuropathy.[31] It is possible that trans-synaptic degeneration triggered by retinal ganglion cell death in both glaucoma and optic neuropathy may lead to white matter diffusion abnormality measured by FA.

Correlation of Unilateral Diffusion MRI with Visual Field

Another novelty of our analysis approach is that we separated the left and right visual fields for comparison. Most prior studies compared MRI data with the left and right eyes but not with left and right visual fields.[13,20,22] The visual pathways are segregated by visual fields after the optic chiasm and thus comparison with visual fields is more appropriate and could improve delineation of neurodegeneration in glaucoma. Standard clinical visual field tests evaluate one eye at a time. There are several methods to derive binocular view from monocular data typically used in clinical settings.[27,28,41] We evaluated two algorithms: "mean" and "best" location of the visual field maps using glaucoma PSD scores. The correlation results from the two methods were not statistically different from each other and thus only the results from the "mean" method were presented. Although there is no ideal way to generate binocular hemifield visual and RNFL scores from monocular data, previous studies have shown this method to combine monocular visual field provides good agreement for comparison with binocular fields.[27,28] Nelson-Quigg et al. found the "best" method was better than the "mean" method to derive binocular visual fields from monocular data.[28] Asymmetric damages between the two eyes could confound the correlation results. It is possible that the "best" method might underestimate corresponding brain degeneration in the case of asymmetric field deficits between eyes. We found the "best" and "mean" methods were tightly correlated and thus had similar correlation with the MRI data. For patients with unilateral damage, one method may be a more appropriate than the other to generate binocular visual field scores and RNFL for comparison to brain degeneration, but this needs further investigation.

Nonetheless, using this method, we found no significant correlation between MRI parameters (i.e., volume and FA, etc) with RNFL thickness, while FA and RD did correlate with visual fields. For the optic radiation, FA had a significant positive correlation with contralateral field scores with visual field score. Previous studies have demonstrated that FA of the optic radiation were significantly correlated with glaucoma stages,[20] optic nerve head damage, and mean visual field score of both eyes.[22] Our results are in agreement with these findings and further underscore the notation that the FA values of the optic radiation could be used to evaluate the severity of visual field loss in glaucoma by separating left and right visual fields. For the optic tract, there was no significant correlation between contralateral field deficits and diffusion parameters. A possible reason for the lack of correlation could be that the optic tract is comparatively small (relative to the optic radiation) and contains fewer neuron bundles leading to lower sensitivity.[30]

We found no significant correlation between RNFL thickness with any MRI parameters (i.e., volume and occur only after a substantial number of retinal ganglion cells have already died and often at later stages of glaucoma,[2–5] whereas thinning of the RNFL may occur at early stage with normal visual field function.[42] Thus, it is possible that the absence of correlation between structural and functional changes could be due to in part that our population included mostly mild to moderate POAG participants. Structure-function correlation likely becomes more apparent at more severe POAG stages. Second, it is also possible that the large inherent inter-subject variability (scattering) in RNFL thickness and MRI parameters could contribute to the lack of correlation. Additionally, combination of RNFL thickness

between two eyes has not been reported to our knowledge, in contrast to visual fields, so it could be that combining thicknesses is not straightforward. Finally, the small sample sizes in our study could contribute to the lack of correlation.

In sum, multimodal MRI could complement standard clinical eye examination by providing added value and unique information about neurodegeneration in the brain that contributes to glaucoma pathogenesis and progression.

Limitations and future directions

There are several limitations of this study. The number of subjects was relatively small although it is typical for many similar MRI-based studies. We expect that with a larger sample sizes, some of the trends in diffusion parameters, and their correlations with vision field scores will likely become statistically significant. We do not have data on the duration and stability of glaucoma for all our participants. The small sample sizes also precluded such analysis. Future studies should include correlation with duration and stability of glaucoma with larger sample sizes.

The dynamic range of disease severity was narrow as the patients had mild or moderate glaucoma. Although these results indicate that neurodegenerative changes occur in the brain even in mild to moderate glaucoma, inclusion of severe glaucoma patients would help to confirm the link between visual field loss and brain atrophy. Future longitudinal studies of POAG by MRI could help to evaluate the progression of brain atrophy and its relation with retina damage progression in patients. Although our spatial resolution is high compared to most previous DTI studies of glaucoma, further improving spatial resolution as well as using image acquisition with less spatial distortion (i.e., non-echo planar imaging acquisition) would help to improve sensitivity. Advanced diffusion method, such as high angular resolution diffusion method, could be used to resolve crossing fibers at the optic chiasm and provide more information of glaucoma damage to the optic nerve and optic tract. The MRI data could not be separated into regions corresponding to the left or right eye; therefore it is possible that the asymmetry between the two eyes could confound the correlation results. Many POAG patients show asymmetric damage around the horizontal midline[43] and thus subdividing white matter tracts with upper and lower visual field could provide additional information.

Conclusion

This study evaluated glaucomatous damage along visual pathway of the brain using novel analysis approaches of volumetric and diffusion tensor MRI. We found various regional abnormalities along the entire visual pathway in the brain. Some of the MRI indices are more sensitive than others in detecting these abnormalities. By comparing glaucomatous visual field loss from the left and right hemifields (instead of left and right eyes), white-matter changes are correlated with the corresponding visual field loss. These findings support the hypothesis that improved analysis of MRI enables improved substructural delineation of neurodegenerative pathogenesis in the brain visual pathways in glaucoma. If neurodegeneration contributes to glaucomatous progression, then treatment strategies for glaucoma needs to consider neuroprotection of the brain to preserve visual function.

Acknowledgments

References

1. Allingham, RR., Damji, K., Freedman, S., Moroi, S., Shafranov, G. Shields' textbook of glaucoma. Philadelphia: Lippincott Willliams & Wilkins; 2005.

2. Kerrigan-Baumrind LA, Quigley HA, Pease ME, Kerrigan DF, Mitchell RS. Number of ganglion cells in glaucoma eyes compared with threshold visual field tests in the same persons. Invest Ophthalmol Vis Sci. 2000; 41:741–748. [PubMed: 10711689]

3. Quigley HA, Addicks EM, Green WR. Optic nerve damage in human glaucoma. III. Quantitative correlation of nerve fiber loss and visual field defect in glaucoma, ischemic neuropathy, papilledema, and toxic neuropathy. Arch Ophthalmol. 1982; 100:135–146. [PubMed: 7055464]

4. Smith EL 3rd, Hung LF, Harwerth RS. Developmental visual system anomalies and the limits of emmetropization. Ophthalmic Physiol Opt. 1999; 19:90–102. [PubMed: 10615445]

5. Limb GA, Martin KR, Res SAPO. Current Prospects in Optic Nerve Protection and Regeneration: Sixth ARVO/Pfizer Ophthalmics Research Institute Conference. Invest Ophth Vis Sci. 2011; 52:5941–5954.

6. AGIS. The Advanced Glaucoma Intervention Study (AGIS): 7. The relationship between control of intraocular pressure and visual field deterioration. The AGIS Investigators. Am J Ophthalmol. 2000; 130:429–440. [PubMed: 11024415]

7. Coleman AL, Miglior S. Risk factors for glaucoma onset and progression. Surv Ophthalmol. 2008; 53(Suppl 1):S3–10. [PubMed: 19038621]

8. Yucel YH, Zhang Q, Weinreb RN, Kaufman PL, Gupta N. Atrophy of relay neurons in magno- and parvocellular layers in the lateral geniculate nucleus in experimental glaucoma. Invest Ophthalmol Vis Sci. 2001; 42:3216–3222. [PubMed: 11726625]

9. Yücel Y. Effects of retinal ganglion cell loss on magno-, parvo-, koniocellular pathways in the lateral geniculate nucleus and visual cortex in glaucoma. Progress in Retinal and Eye Research. 2003; 22:465–481. [PubMed: 12742392]

10. Whitmore AV, Libby RT, John SW. Glaucoma: thinking in new ways-a role for autonomous axonal self-destruction and other compartmentalised processes? Prog Retin Eye Res. 2005; 24:639–662. [PubMed: 15953750]

11. Gupta N, Ang LC, Noel de Tilly L, Bidaisee L, Yucel YH. Human glaucoma and neural degeneration in intracranial optic nerve, lateral geniculate nucleus, and visual cortex. Br J Ophthalmol. 2006; 90:674–678. [PubMed: 16464969]

12. Howell GR, Soto I, Libby RT, John SW. Intrinsic axonal degeneration pathways are critical for glaucomatous damage. Experimental neurology. 2013; 246:54–61. [PubMed: 22285251]

13. Lee JY, Jeong HJ, Lee JH, Kim YJ, Kim EY, Kim YY, Ryu T, Cho ZH, Kim YB. An investigation of lateral geniculate nucleus volume in patients with primary open-angle glaucoma using 7 tesla magnetic resonance imaging. Invest Ophthalmol Vis Sci. 2014; 55:3468–3476. [PubMed: 24722700]

14. Gupta N, Greenberg G, de Tilly LN, Gray B, Polemidiotis M, Yucel YH. Atrophy of the lateral geniculate nucleus in human glaucoma detected by magnetic resonance imaging. Br J Ophthalmol. 2009; 93:56–60. [PubMed: 18697810]

15. Zikou AK, Kitsos G, Tzarouchi LC, Astrakas L, Alexiou GA, Argyropoulou MI. Voxel-based morphometry and diffusion tensor imaging of the optic pathway in primary open-angle glaucoma: a preliminary study. AJNR Am J Neuroradiol. 2012; 33:128–134. [PubMed: 22116110]

16. Chen WW, Wang N, Cai S, Fang Z, Yu M, Wu Q, Tang L, Guo B, Feng Y, Jonas JB, Chen X, Liu X, Gong Q. Structural brain abnormalities in patients with primary open-angle glaucoma: a study with 3T MR imaging. Invest Ophthalmol Vis Sci. 2013; 54:545–554. [PubMed: 23258150]

17. Hernowo AT, Boucard CC, Jansonius NM, Hooymans JM, Cornelissen FW. Automated morphometry of the visual pathway in primary open-angle glaucoma. Invest Ophthalmol Vis Sci. 2011; 52:2758–2766. [PubMed: 21398286]

18. Garaci FG, Bolacchi F, Cerulli A, Melis M, Spano A, Cedrone C, Floris R, Simonetti G, Nucci C. Optic nerve and optic radiation neurodegeneration in patients with glaucoma: in vivo analysis with 3-T diffusion-tensor MR imaging. Radiology. 2009; 252:496–501. [PubMed: 19435941]

19. El-Rafei A, Engelhorn T, Warntges S, Dorfler A, Hornegger J, Michelson G. Glaucoma classification based on visual pathway analysis using diffusion tensor imaging. Magn Reson Imaging. 2013; 31:1081–1091. [PubMed: 23751976]

20. Dai H, Yin D, Hu C, Morelli JN, Hu S, Yan X, Xu D. Whole-brain voxel-based analysis of diffusion tensor MRI parameters in patients with primary open angle glaucoma and correlation with clinical glaucoma stage. Neuroradiology. 2013; 55:233–243. [PubMed: 23223846]

21. Chang ST, Xu J, Trinkaus K, Pekmezci M, Arthur SN, Song SK, Barnett EM. Optic nerve diffusion tensor imaging parameters and their correlation with optic disc topography and disease severity in adult glaucoma patients and controls. J Glaucoma. 2014; 23:513–520. [PubMed: 23632406]

22. Michelson G, Engelhorn T, Warntges S, El Rafei A, Hornegger J, Doerfler A. DTI parameters of axonal integrity and demyelination of the optic radiation correlate with glaucoma indices. Graefes Arch Clin Exp Ophthalmol. 2013; 251:243–253. [PubMed: 22366916]

23. Schiff D, Cohen B, Buttner-Ennever J, Matsuo V. Effects of lesions of the nucleus of the optic tract on optokinetic nystagmus and after-nystagmus in the monkey. Exp Brain Res. 1990; 79:225–239. [PubMed: 2323371]

24. Yeatman JD, Dougherty RF, Myall NJ, Wandell BA, Feldman HM. Tract profiles of white matter properties: automating fiber-tract quantification. PLoS One. 2012; 7:e49790. [PubMed: 23166771]

25. The American Academy of Ophthalmology Preferred Practice Pattern Glaucoma Panel: Primary Open-Angle Glaucoma Preferred Practice Pattern® Guidelines. American Academy of Ophthalmology. 2015; 123

26. Mills RP, Budenz DL, Lee PP, Noecker RJ, Walt JG, Siegartel LR, Evans SJ, Doyle JJ. Categorizing the stage of glaucoma from pre-diagnosis to end-stage disease. Am J Ophthalmol. 2006; 141:24–30. [PubMed: 16386972]

27. Crabb DP, Viswanathan AC, McNaught AI, Poinoosawmy D, Fitzke FW, Hitchings RA. Simulating binocular visual field status in glaucoma. Br J Ophthalmol. 1998; 82:1236–1241. [PubMed: 9924324]

28. Nelson-Quigg JM, Cello K, Johnson CA. Predicting binocular visual field sensitivity from monocular visual field results. Invest Ophthalmol Vis Sci. 2000; 41:2212–2221. [PubMed: 10892865]

29. Mukherjee P, Chung SW, Berman JI, Hess CP, Henry RG. Diffusion tensor MR imaging and fiber tractography: technical considerations. AJNR Am J Neuroradiol. 2008; 29:843–852. [PubMed: 18339719]

30. Andrews TJ, Halpern SD, Purves D. Correlated size variations in human visual cortex, lateral geniculate nucleus, and optic tract. J Neurosci. 1997; 17:2859–2868. [PubMed: 9092607]

31. Ogawa S, Takemura H, Horiguchi H, Terao M, Haji T, Pestilli F, Yeatman JD, Tsuneoka H, Wandell BA, Masuda Y. White matter consequences of retinal receptor and ganglion cell damage. Invest Ophthalmol Vis Sci. 2014; 55:6976–6986. [PubMed: 25257055]

32. Yu L, Yin X, Dai C, Liang M, Wei L, Li C, Zhang J, Xie B, Wang J. Morphologic changes in the anterior and posterior subregions of V1 and V2 and the V5/MT+ in patients with primary open-angle glaucoma. Brain Res. 2014; 1588:135–143. [PubMed: 25199592]

33. Dickerson BC, Feczko E, Augustinack JC, Pacheco J, Morris JC, Fischl B, Buckner RL. Differential effects of aging and Alzheimer's disease on medial temporal lobe cortical thickness and surface area. Neurobiol Aging. 2009; 30:432–440. [PubMed: 17869384]

34. Ptito M, Schneider FC, Paulson OB, Kupers R. Alterations of the visual pathways in congenital blindness. Exp Brain Res. 2008; 187:41–49. [PubMed: 18224306]

35. Park HJ, Lee JD, Kim EY, Park B, Oh MK, Lee S, Kim JJ. Morphological alterations in the congenital blind based on the analysis of cortical thickness and surface area. Neuroimage. 2009; 47:98–106. [PubMed: 19361567]

36. Chen Z, Lin F, Wang J, Li Z, Dai H, Mu K, Ge J, Zhang H. Diffusion tensor magnetic resonance imaging reveals visual pathway damage that correlates with clinical severity in glaucoma. Clin Experiment Ophthalmol. 2013; 41:43–49. [PubMed: 22712443]

37. Schmidt MA, Mennecke A, Michelson G, Doerfler A, Engelhorn T. DTI analysis in patients with primary open-angle glaucoma: impact of registration on Voxel-Wise statistics. PLoS One. 2014; 9:e99344. [PubMed: 24901535]

38. Wassermann D, Rathi Y, Bouix S, Kubicki M, Kikinis R, Shenton M, Westin CF. White matter bundle registration and population analysis based on Gaussian processes. Inf Process Med Imaging. 2011; 22:320–332. [PubMed: 21761667]

39. Alexander AL, Lee JE, Lazar M, Field AS. Diffusion tensor imaging of the brain. Neurotherapeutics. 2007; 4:316–329. [PubMed: 17599699]

40. Tang YY, Lu Q, Fan M, Yang Y, Posner MI. Mechanisms of white matter changes induced by meditation. Proc Natl Acad Sci U S A. 2012; 109:10570–10574. [PubMed: 22689998]

41. Crabb DP, Viswanathan AC. Integrated visual fields: a new approach to measuring the binocular field of view and visual disability. Graefes Arch Clin Exp Ophthalmol. 2005; 243:210–216. [PubMed: 15806374]

42. Bowd C, Zangwill LM, Berry CC, Blumenthal EZ, Vasile C, Sanchez-Galeana C, Bosworth CF, Sample PA, Weinreb RN. Detecting early glaucoma by assessment of retinal nerve fiber layer thickness and visual function. Invest Ophthalmol Vis Sci. 2001; 42:1993–2003. [PubMed: 11481263]

43. Mandava S, Zulauf M, Zeyen T, Caprioli J. An evaluation of clusters in the glaucomatous visual field. Am J Ophthalmol. 1993; 116:684–691. [PubMed: 8250069]
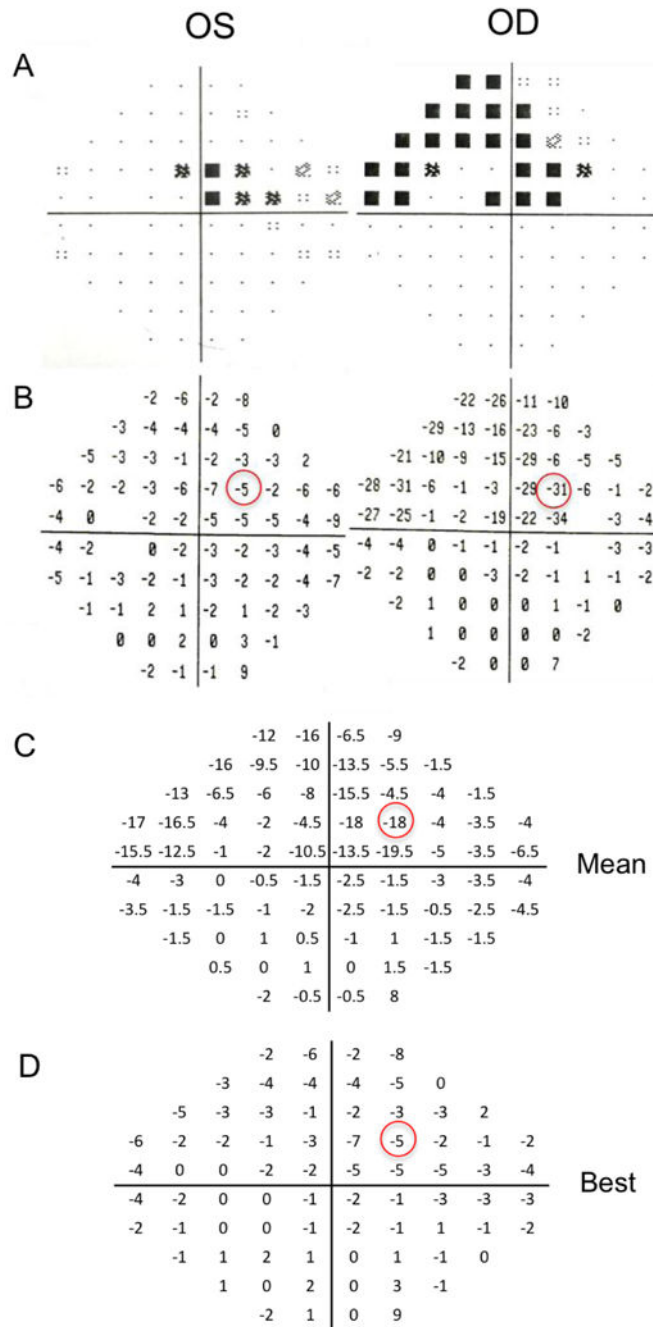
Figure 1.
Monocular perimetry data from a POAG patient. The (A) gray scale and (B) pattern standard deviation (PSD) scores of each eye. For each patient, the PSD values of right and left eyes were combined point by point by taking either the (C) "mean" or the (D) "best" of the two eyes to obtain binocular visual fields. The binocular PSD scores were then separated to left and right visual fields and averaged for each field for quantitative analysis. Darker shade and more negative values indicate worse visual deflect.
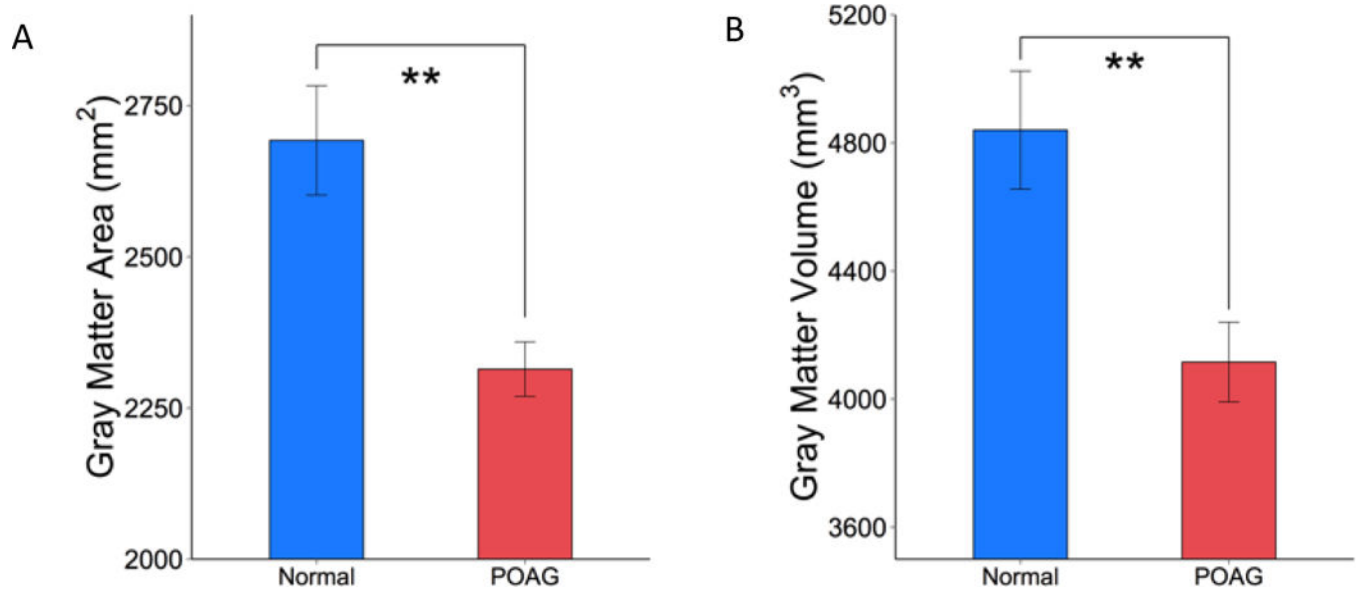
Figure 2.
Group comparison of (A) area and (B) volume of the primary visual cortex V1 from normal controls and POAG subjects. Mean ± SEM. ** p < 0.01
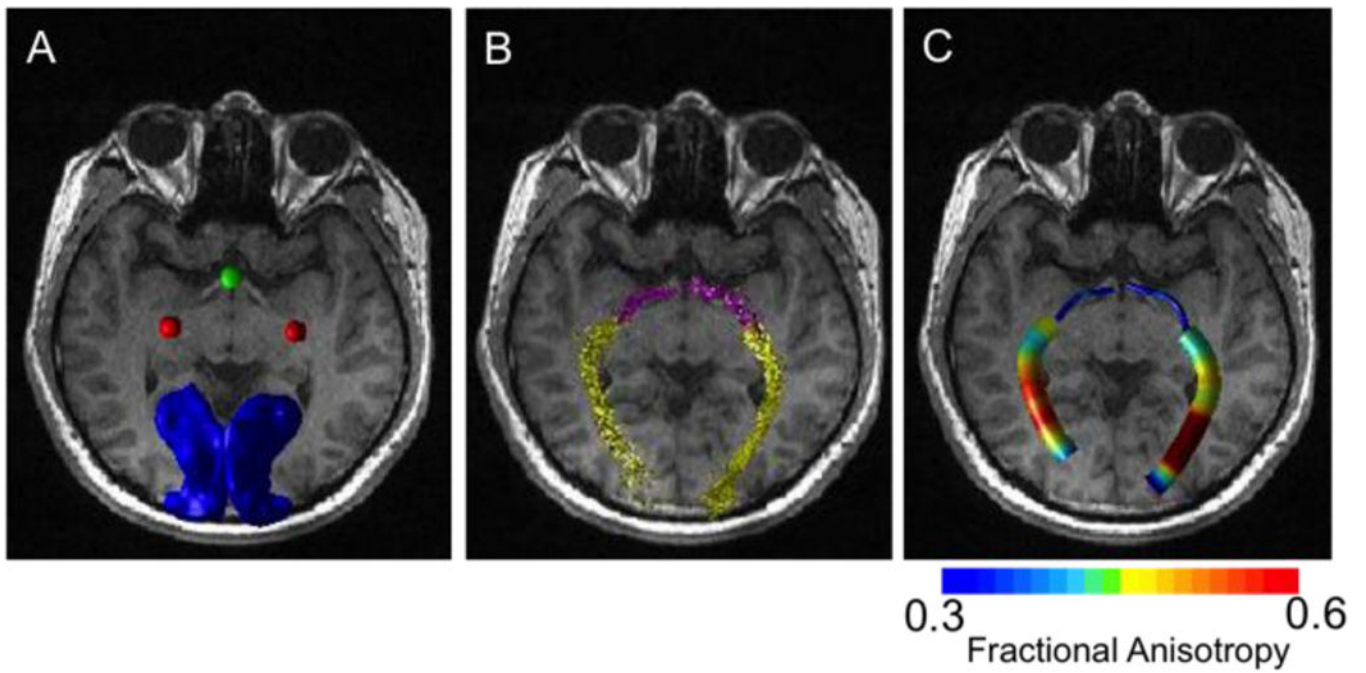
Figure 3.
(A) Typical ROI seeds used for fiber tracking overlaid on an anatomical image from a representative normal subject: optic chiasm[3], lateral geniculate nucleus (red), and V1 (blue). (B) Fiber tracts of the optic tract (pink) and optic radiation (yellow). (C) The corresponding fractional anisotropy along the fiber tracts.
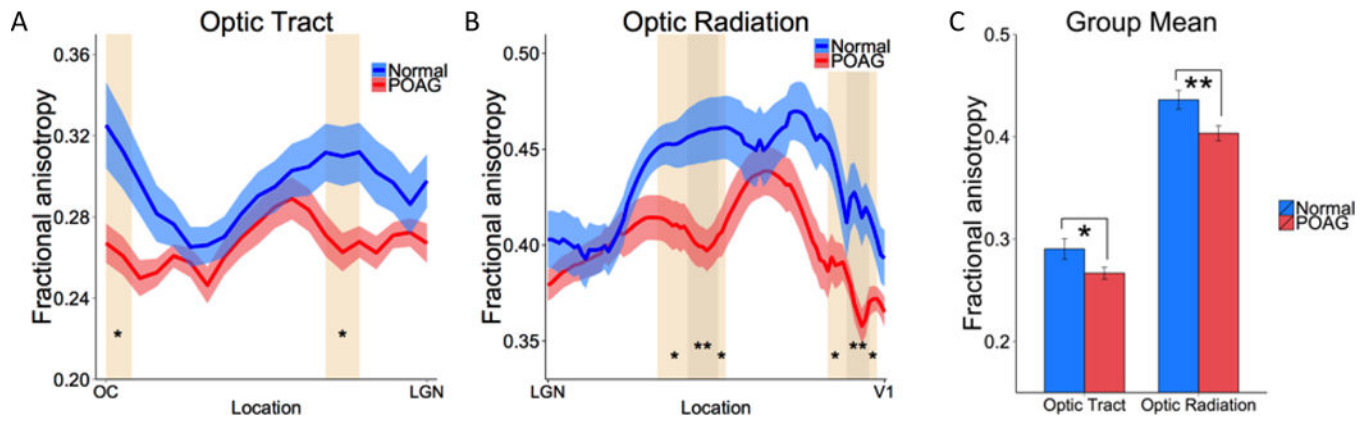
Figure 4.
Group average fractional anisotropy profiles along the (A) optic tract and (B) optic radiation from normal control and POAG subjects. (C) Average fractional anisotropy of both structures from normal and POAG subjects. The shaded areas and error bars represent SEM, with * p < 0.05, ** p < 0.01 indicating statistical significances.
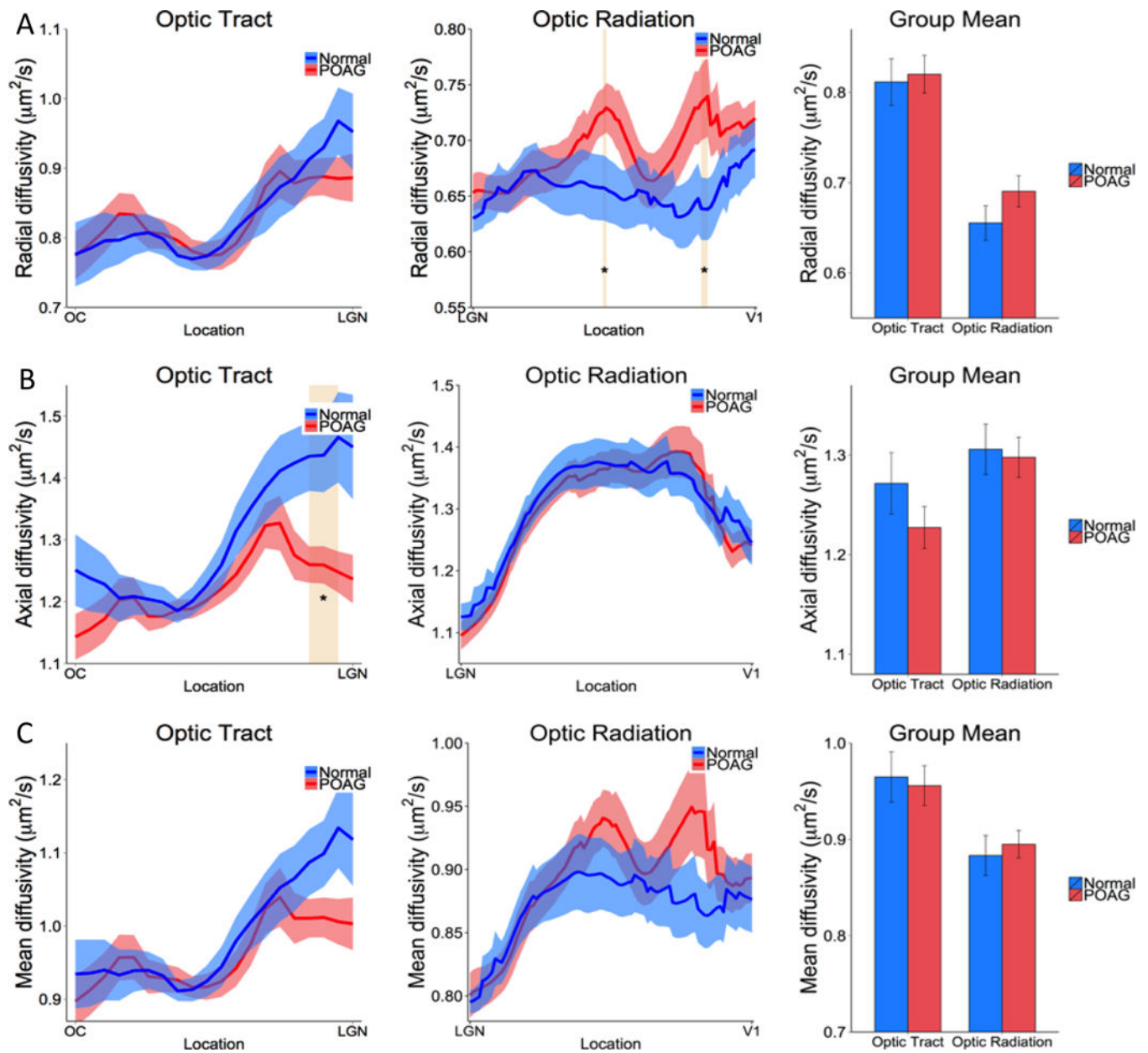
Figure 5.
Group (A) radial, (B) axial and (C) mean diffusivity profiles along the optic tract and optic radiation and their averaged values from normal and POAG subjects. The shaded areas and error bars represent SEM, with * p < 0.05 indicating statistical significances.

Table 1

Demographic and clinical data of individual POAG patients. Visual field (pattern standard deviation, PSD), intraocular pressure (IOP), and retinal nerve fiber layer (RNFL) thickness are shown for right[42] and left (OS) eyes.

No	Sex	Age	Visual Field (dB)		IOP (mmHg)		RNFL (μm)	
			OD PSD	OS PSD	OD	OS	OD	OS
1	F	58	−1.94	−3.31	14	15	77 *	66 **
2	F	65	−2.32	−1.3	15	16	104	113
3	F	59	−1.6	−4.75	12	18	88	76 *
4	M	58	−12.92	−9.58	14	16	44 **	69 **
5	M	36	−1.3	−3.2	31	51	80 *	67 **
6	M	60	−5.33	−6.21	11	11	60 **	72 **
7	M	72	−7.49	−2.54	10	10	73 **	92
8	F	63	−1.65	−2.02	14	15	80 *	82
9	F	63	−10.43	−7.97	17	16	71 **	78 *
10	F	58	−3.83	−1.35	15	14	97	95
11	F	68	−1.94	−1.67	19	19	78 *	97

*
p<0.05,

**
p<0.01 indicates RNFL thickness of inner cycle significantly, different from normative data set.